Table 1. Comparison best fit parameters of different model and rheologies, for an ice stream age of 2000 years. Arrows show the change from original parameters in the main paper to the best fit parameters for a 2000 year old ice stream. Parameters in italics were chosen by fitting, blank entries mean the paramater is not included in the model.

Model/rheology	α_D	α_S	$\tilde{\lambda}$	$\tilde{\beta}$	E_{cc}	E_{ca}	n
Taylor	1	0	*0.03 → 0.0*	0			
Sachs	0	1	*0.32 → 0.25*	0	1	10^2	
GOLF	*0 → 0*	*1.15 → 1.0*	*0.45 → 0.3*	0	1	10^2	
Rathmann w/ Full η	*0 → 0*	*1.47 → 1.5*	*0.49 → 0.45*	0	1	10^2	3
Rathmann w/ $\eta = (\boldsymbol{\tau} : \boldsymbol{\tau})^{(n-1)/2}$	*0 → 0*	*1.1 → 1.0*	*0.36 → 0.25*	0	1	10^2	
CAFFE w/ $E_{\max} = 10$, $E_{\min} = 0.1$	*0 → 0*	*1.1 → 1.1*	*0.36 → 0.36*	0			
Estar/Glen	*2.6 → 2.0*	0	*0.32 → 0.2*	0			

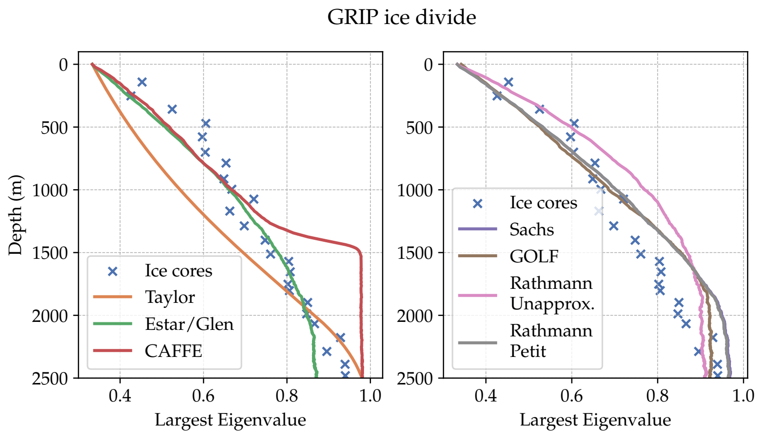

Figure S1. Evolution of largest (vertical) eigenvalue of the second-order orientation tensor **A** at the GRIP drill site (an ice divide) with depth, for a 2000 year old ice stream. Only the largest eigenvalue is shown as the fabric has rotational symmetry about the vertical, so the other two eigenvalues are equal. Measurements from ice cores are plotted as crosses, showing an increase with depth. Model results are plotted as lines, and have been split across two subplots to aid readability. The right hand plot shows the tensorial rheologies.

Section S1: Best fit parameters for 2000yr old ice stream

Table 1 shows the best fit parameters for a 2000 year old ice stream. The original parameters are also shown with arrows showing the original → young ice stream. Generally these is a trend for the amount of fabric diffusion (λ) required to reduce. Figs. S1, S2, S3 show figures from the main paper reproduced with the 2000 year old ice stream. The overall ranking of the rheologies/models does not change. Generally there is worse fit at the ice divide and better fit in the ice stream.

Section S2: Parameter sensitivity study

In this section of the supplement we perform a parameter sensitivity study for parameter and model combination. To recall, the model can be described by:

$$\frac{df(\boldsymbol{n})}{dt} = -\nabla^* \cdot (f\boldsymbol{v}) + \lambda \nabla^{*2}(f) + \beta f(s' - \langle s' \rangle), \tag{1}$$

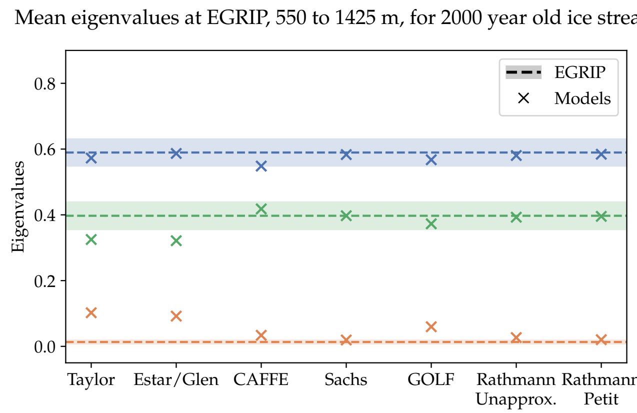

Figure S2. This figure shows, for each model/rheology, the mean eigenvalues over a depth of 550 to 1425 m, for a 2000 year old ice stream. Colours indicate the different eigenvalues. These are shown as crosses. A horizontal line shows the 'true' observations from EGRIP at this depth, with the dashed line showing the mean eigenvalues and the shaded region corresponding to $\pm$ 1 standard deviation.

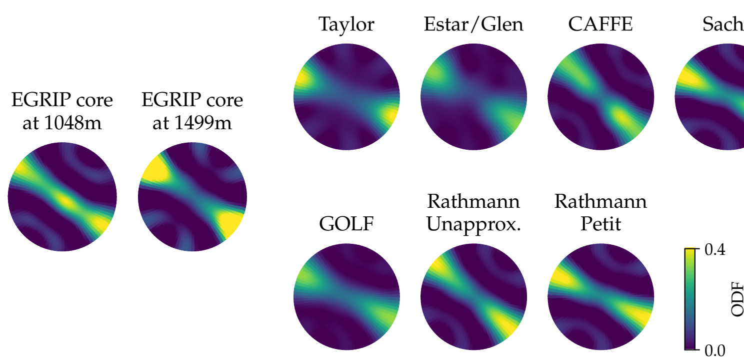

Figure S3. Comparison of pole figures, for all models and measured from an ice core at two depths for a 2000 year old ice stream. The pole figure shows a hemisphere of the orientation distribution function, which is sufficient to show all the information. Pole figures are shown looking vertically downwards, with North at the top. For example, the observed fabric at EGRIP at 1048 m shows that almost all grains lie close to a plane normal to the North-East direction.

$$\boldsymbol{v}(\boldsymbol{n}) = \boldsymbol{\omega} \cdot \boldsymbol{n} - \alpha_D(\dot{\boldsymbol{\varepsilon}} \cdot \boldsymbol{n} - (\dot{\boldsymbol{\varepsilon}} : \boldsymbol{nn})\boldsymbol{n}) - \alpha_S \iota(\hat{\boldsymbol{\tau}} \cdot \boldsymbol{n} - (\hat{\boldsymbol{\tau}} : \boldsymbol{nn})\boldsymbol{n}), \tag{2}$$

where α_D controls the effect of lattice rotation due to deformation, α_S controls the effect of lattice rotation due to stress, dependent on each model/rheology. $\tilde{\lambda}$ controls the effect of diffusion or Brownian motion, modelling rotational recrystallization. $\tilde{\beta}$ controls the effect of migration recrystallization. E_{cc} and E_{ca} control the enhancement of a grain parallel and perpendicular to the c-axis respectively. Finally n controls a power-law response

For each parameter we explore the effect on the average eigenvalues predicted at EGRIP, over the same depth explored in Fig. 7 and Fig. 9 in the main paper. This is shown first for α_D in Fig. S4. As this parameter does not link to any rheology, only 1 plot is shown. The other parameters are shown at the bottom of the figure. For this, $\alpha_S = 0$ was used. The important thing to highlight is that even for very large values of α_D, a girdle fabric is never predicted.

Figure S5 shows the effect of varying the parameter α_S. As this directly controls effect the lattice rotation of stress, and the stress is found through the rheology, different responses are found for each rheology. The response for Glen's rheology is

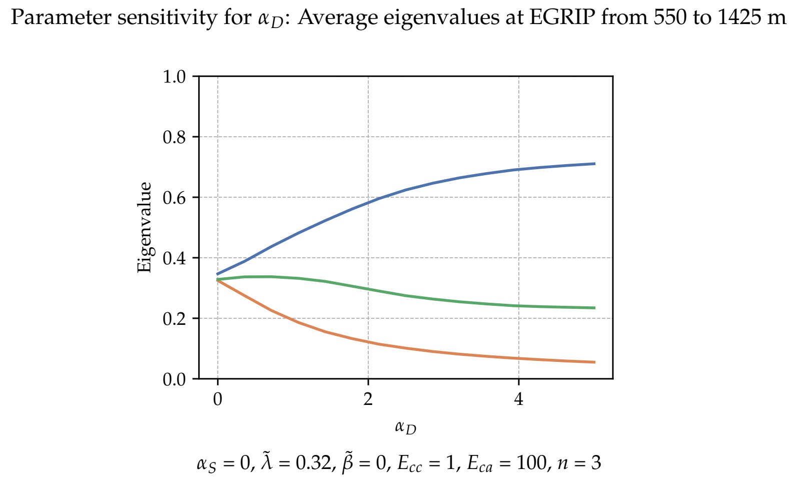

Figure S4. Sensitivity of the Sachs rheology with the best fit parameters described in the main paper (and shown under the figure) to changes in the parameter α_D, controlling the effect of lattice rotation due to deformation. The plot shows the three eigenvalues at the EGRIP ice stream, averaged over a depth of 550 to 1425 m. The other parameters are kept constant. Only 1 model/rheology is shown in this figure (in contrast to the ones below) as the parameter α_D is not linked to the stress, found through the rheology, so the change is the same for each model/rheology.

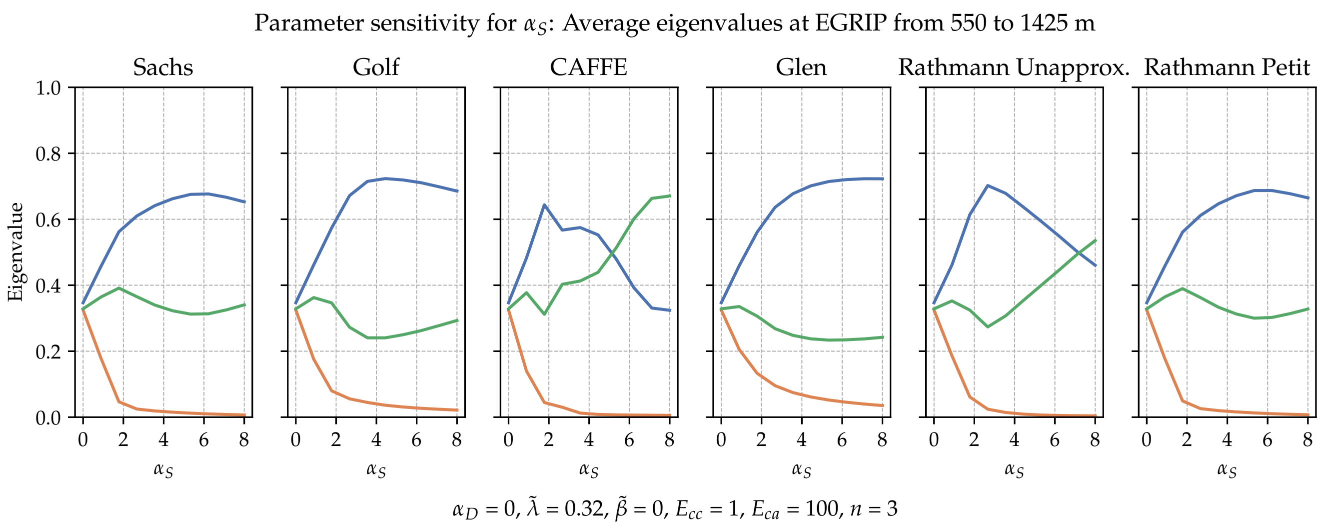

Figure S5. Sensitivity of a range of rheologies to changes in α_S, controlling the effect of lattice rotation due to stress, found through the rheology. The plot shows the three eigenvalues at the EGRIP ice stream, averaged over a depth of 550 to 1425 m. The other parameters are kept constant at the value values shown below.

identical to Fig. S4 as for this rheology $\hat{\boldsymbol{\tau}} = \dot{\boldsymbol{\varepsilon}}$. The other rheologies have more varied responses and are sensitive to changes in α_S, though there is no physical justification for values of α_S much greater than 1.

The effect of the parameter $\tilde{\lambda}$, controlling the effect of rotational recrystallization modelled through Brownian motion of orientations or diffusion of orientation concentrations, is shown in Fig. S6. Like α_D, this does not depend on the rheology

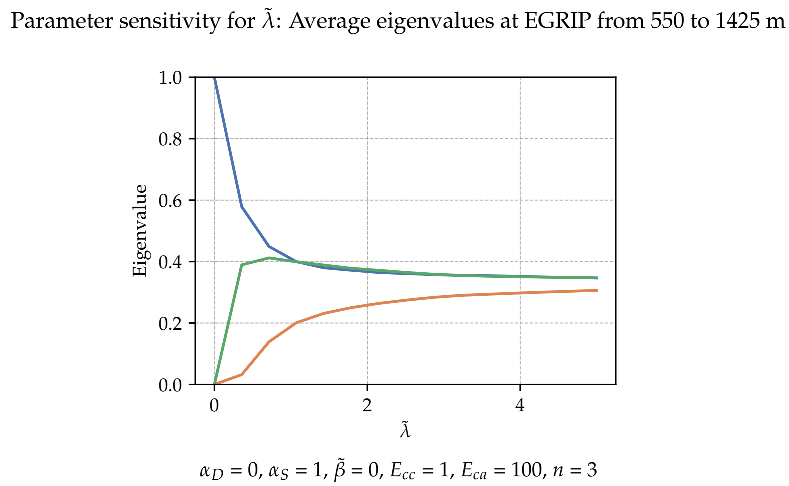

Figure S6. Sensitivity of the Sachs rheology with the best fit parameters described in the main paper (and shown under the figure) to changes in the parameter $\tilde{\lambda}$, controlling the effect of rotational recrystallization, modelled as a diffusion of the fabric. The plot shows the three eigenvalues at the EGRIP ice stream, averaged over a depth of 550 to 1425 m. The other parameters are kept constant. Only 1 model/rheology is shown in this figure (in contrast to the ones below) as the parameter α_D is not linked to the stress, found through the rheology, so the change is the same for each model/rheology.

used. The model is clearly very sensitive to this parameter. For $\tilde{\lambda} = 0$, with no diffusion a single maximum is produced. The girdle fabric seen in he results is only produced over a range of 0.2 to $\tilde{1}$.5. For large values of $\tilde{\lambda}$, the fabric tends to isotropic (all eigenvalues $= 1/3$).

We also show the sensitivity of the different models to β in Fig. S7, controlling the effect of migration recrystallization, which we set to 0 in the main paper. When comparing to Richards et al. (2021) the parameters in that paper should be multiplied by a factor of 5 to compare to Fig. S7.

The sensitivity of E_{cc} is shown in Fig. S8. E_{cc} represents the enhancement of grain parallel to the c-axis. We show this figure for completeness, as there no evidence to suggest $E_{cc} \neq 1$ (Gillet-Chaulet et al., 2005).

For E_{ca}, controlling the enhancement of ice in shear, we explore the parameter sensitivity for the 4 anisotropic rheologies this parameter enters. This is shown over the range of 1 to 10^5 for the Sachs and Rathmann rheologies, but only for 10 to 100 for the GOLF rheology, as it is only tabulated at these values. There is little sensitivity for the GOLF rheology over the range explored. For the Sachs and Rathmann rheologies, there is an asymptotic behaviour as $E_{ca} \to \infty$, with little change for $E_{ca} > 10^2$.

The sensitivity to n is shown in Fig. S10. As only the fabric predictions only depend on n for Rathmann's unapproximated rheology, only this is shown. $n = 1$ for this rheology gives the same response as Rathmann's rheology with the Petit approximation. Above $n = 2$, the fabric predictions are insensitive to the n value. The unapproximated Rathmann rheology with $n = 1$ gives the same predictions as the Rathmann rheology with Petit approximation.

Finally, we also show the sensitivity of the CAFFE rheology to changes in E_{max} and E_{min} in Fig. S11 and S12. There is strong physical justification for $E_max \approx 10$ so Fig. S11 is shown for completeness. Placidi et al. (2010) state that E_{min} can be chosen freely between 0 and 0.1 but Fig. S12 shows results are clearly sensitive to this.

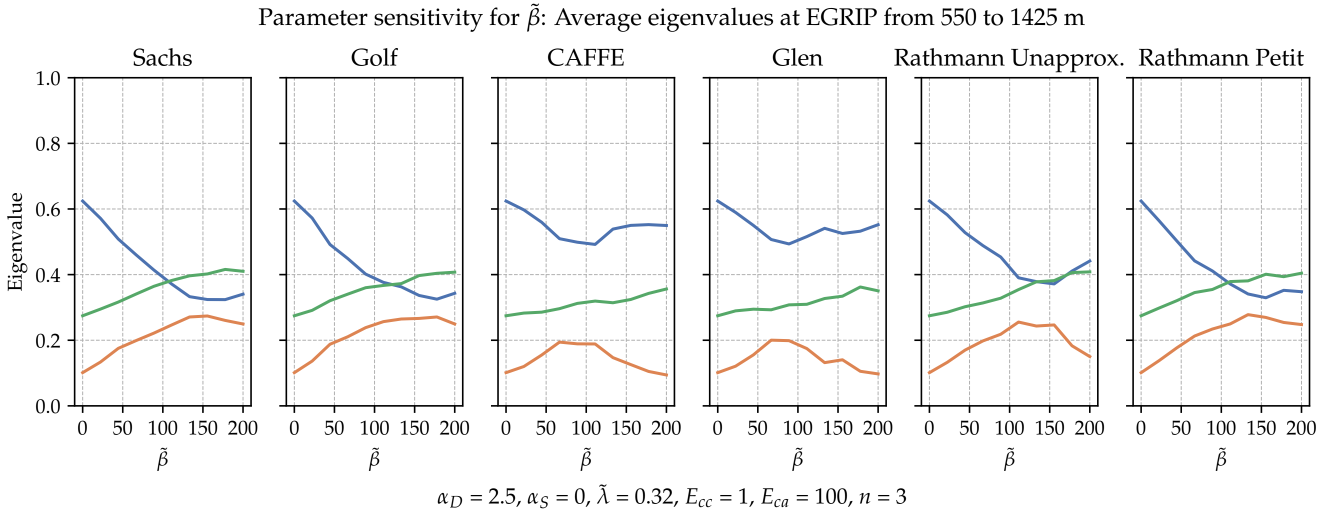

Figure S7. Sensitivity of a range of rheologies to changes in β, controlling the effect of migration recrystallization. The plot shows the three eigenvalues at the EGRIP ice stream, averaged over a depth of 550 to 1425 m. The other parameters are kept constant at the value values shown below.

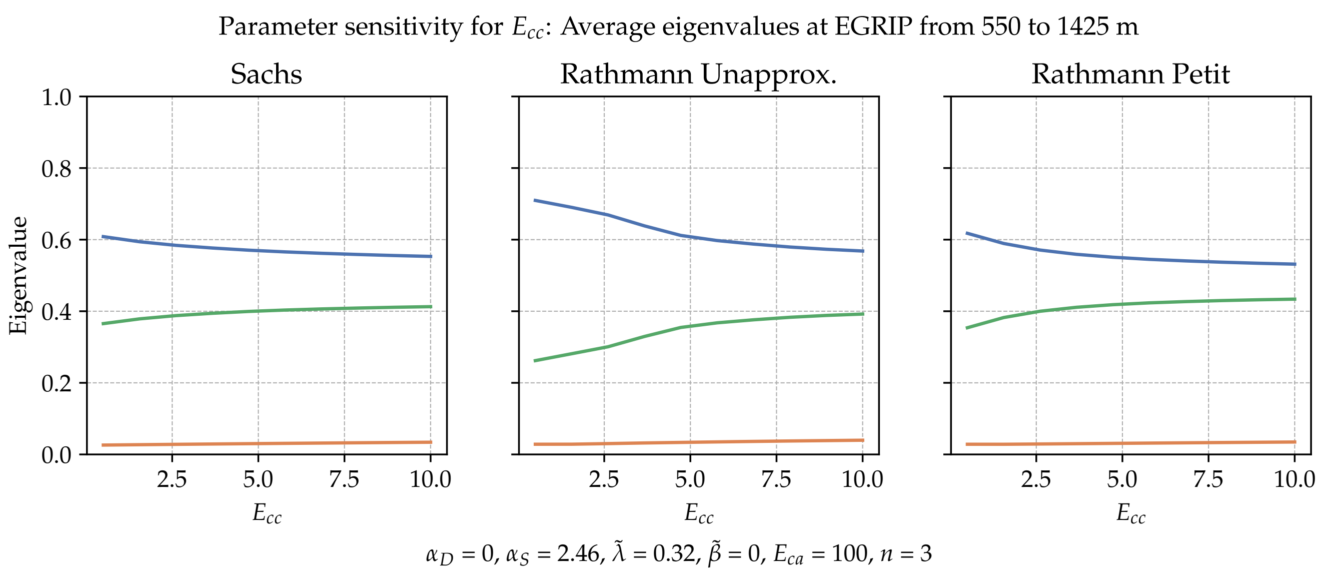

Figure S8. Sensitivity of the Sachs and Rathmann rheologies to changes in E_{cc}, from 1 to 10, controlling the enhancement of a grains rheological response parallel to the c-axis. The plot shows the three eigenvalues at the EGRIP ice stream, averaged over a depth of 550 to 1425 m. The other parameters are kept constant at the value values shown below.

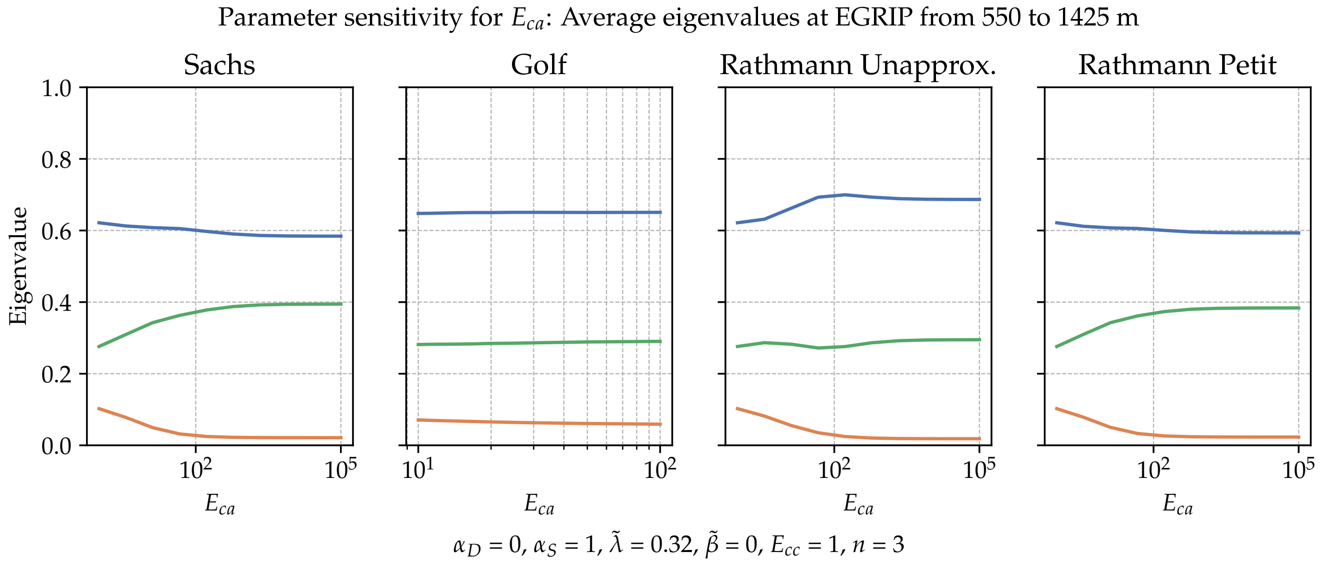

Figure S9. Sensitivity of the anisotropic rheologies to changes in E_{ca}, controlling the enhancement of a grains rheological response perpendicular to the c-axis. The plot shows the three eigenvalues at the EGRIP ice stream, averaged over a depth of 550 to 1425 m. The other parameters are kept constant at the value values shown below. The GOLF rheology is shown over a limited range as it only supports certain values of E_{ca}.

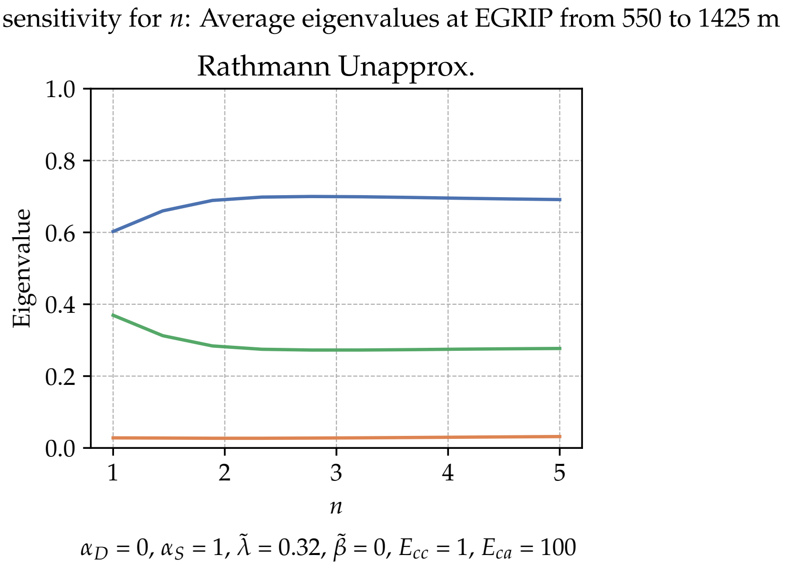

Figure S10. Sensitivity of the unapproximated Rathmann rheology with the parameters shown to changes in power exponent n. Only this rheology is shown as it is the only one with a dependence on the value of n. The plot shows the three eigenvalues at the EGRIP ice stream, averaged over a depth of 550 to 1425 m. The other parameters are kept constant at the value values shown below.

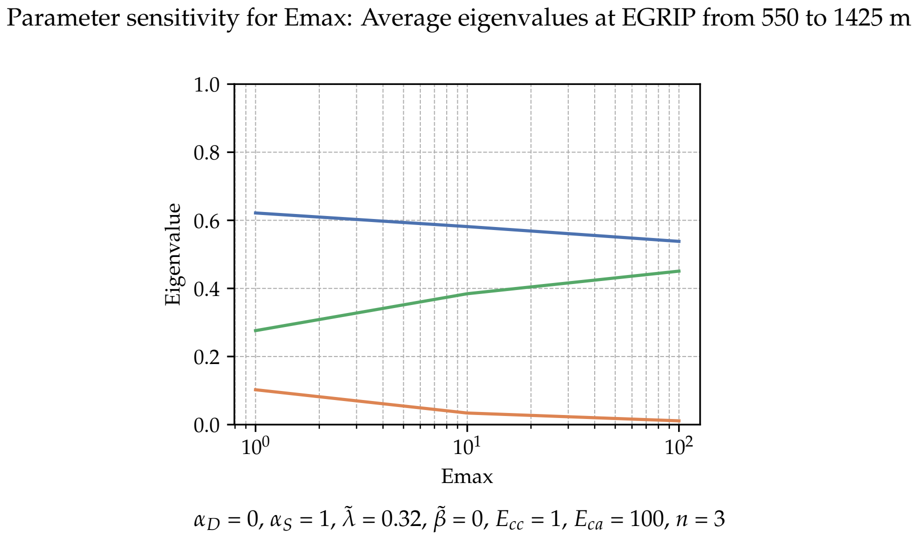

Figure S11. Sensitivity of the CAFFE rheology with the best fit parameters described in the main paper (and shown under the figure) to changes in the parameter E_{max}, controlling the maximum softening in the CAFFE model and set at 10 in the main paper. The plot shows the three eigenvalues at the EGRIP ice stream, averaged over a depth of 550 to 1425 m. The other parameters are kept constant.

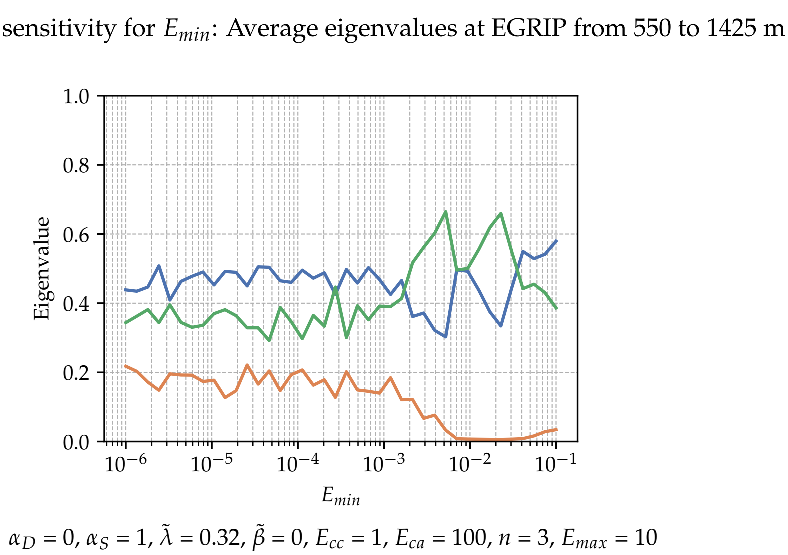

Figure S12. Sensitivity of the CAFFE rheology with the best fit parameters described in the main paper (and shown under the figure) to changes in the parameter E_{min}, controlling the minimum softening in the CAFFE model and set at 0.1 in the main paper. The plot shows the three eigenvalues at the EGRIP ice stream, averaged over a depth of 550 to 1425 m. The other parameters are kept constant.

References

Gillet-Chaulet, F., Gagliardini, O., Meyssonnier, J., Montagnat, M., and Castelnau, O.: A user-friendly anisotropic flow law for ice-sheet modeling, Journal of Glaciology, 51, 3–14, https://doi.org/10.3189/172756505781829584, 2005.

Placidi, L., Greve, R., Seddik, H., and Faria, S. H.: Continuum-mechanical, Anisotropic Flow model for polar ice masses, based on an anisotropic Flow Enhancement factor, Continuum Mechanics and Thermodynamics, 22, 221–237, https://doi.org/10.1007/s00161-009-0126-0, 2010.

Richards, D. H., Pegler, S. S., Piazolo, S., and Harlen, O. G.: The evolution of ice fabrics: A continuum modelling approach validated against laboratory experiments, Earth and Planetary Science Letters, 556, 116 718, https://doi.org/10.1016/j.epsl.2020.116718, 2021.